

Synthesis and enhanced photocatalytic property of La-doped CuO nanostructures by electrodeposition method

Bing Yan¹ · Yongqian Wang¹ · Tingting Jiang¹ · Xiuling Wu¹

Received: 12 January 2016 / Accepted: 28 January 2016 / Published online: 3 February 2016
© Springer Science+Business Media New York 2016

Abstract La-doped CuO nanosheets were prepared through a electrodeposition method in order to enhance their photocatalytic properties. X-ray diffraction pattern (XRD) and field emission scanning electron microscopy (FESEM) with energy dispersive spectroscopy (EDS) demonstrated that La³⁺ entered the crystal lattice of CuO and substituted Cu²⁺ without destroying crystal structures to form petal-like CuO nanostructures. The band gap of doped samples range between 1.10 and 1.30 eV. Better photocatalytic activity for the photodegradation of methyl blue than the pure CuO nanostructures, which is 11.5 % higher than that in undoped CuO.

1 Introduction

Cupric oxide (CuO) is one of the most extensively studied and promising semiconductive materials in electrocatalytic and photocatalytic application due to its redox selectivity, high stability, low cost and easy preparation [1, 2]. Although CuO materials processes excellent physical and chemical properties at nano scale, it has some disadvantages such as easy recombination of electron and hole [3]. In order to enhance the performance of CuO materials, metal deposition, surface modifications, inorganic dye, doping and others are the effective means for modification [4]. Previous works about doping of transition metal ions into CuO lattice have been reported such as In, Mn, Li, Fe, Ni, Zn [5–10]. Few attempts have been found regarding the

use of lanthanum doping in thin films oxides. It is a well recognized for catalysis through the changes it can bring to the surface state of the materials [11]. Because when La ions are entered into the crystals, generated surface defects can hinder the recombination of photo-induced electron-hole pairs to improve the photocatalytic activity. Furthermore, CuO nanostructures are extensively used in various other applications, including gas sensors, nanofluid, photodetectors, field emissions, bio-sensors, supercapacitors, removal of inorganic pollutants, energetic materials (EMs) and photocatalysis [12–20].

In this paper, an attempt is made to study the optical and photocatalytic property of CuO nanostructured film by doping lanthanum via electrodeposition method. The influence of La concentration on nanostructured CuO photocatalysts is investigated by degradation of methylene blue (MB) under UV and visible light illumination. We also explain the reasons for the enhanced photocatalytic performance.

2 Experiment

2.1 Chemicals

All chemicals used in this work were of analytical reagent grade and used as received without further purification. All the aqueous solutions were prepared using deionized water. Conditions were shown in Table 1.

2.2 Preparation of CuO and La-doped CuO nanostructures

The electrodeposition method was employed to synthesize La-doped CuO nanostructures. The ITO conductive glass

✉ Yongqian Wang
cugwyq@126.com

¹ Faculty of Material Science and Chemistry, China University of Geoscience, Wuhan 430074, China

Table 1 The experimental materials and their specifications

Material composition	Norms
Absolute ethyl alcohol	Analytically pure
Acetone	Analytically pure
Glacial acetic acid	w/% ≥ 99.5
Sodium acetate	Purity > 99 %
Copper acetate	Purity > 99 %
	Purity > 99 %
CTAB	Purity > 99 %
ITO	Square resistance $\leq 15/\square$, transmissivity (T %) ≥ 86 %, 2×5 cm

was used as substrate and tailored into square shape with dimensions of $2 \text{ cm} \times 5 \text{ cm}$, which should be cleaned ultrasonically in the order of acetone, absolute ethyl alcohol and distilled water for 15 min, respectively. Then, it was dried in drying oven for spare use. The experimental procedures were simply described as follows. Firstly, 0.1 M sodium acetate (CH_3COONa) and 0.02 M copper acetate ($\text{Cu}(\text{CH}_3\text{COO})_2 \cdot \text{H}_2\text{O}$) were obtained by dissolving 2.7 g CH_3COONa , 0.8 g $\text{Cu}(\text{CH}_3\text{COO})_2 \cdot \text{H}_2\text{O}$ and 0.03 g CTAB in 200 ml de-ionized water under constant stirring at 25°C . An appropriate amount of lanthanum nitrate ($\text{La}(\text{NO}_3)_3 \cdot 6\text{H}_2\text{O}$) was introduced into the above solution. Glacial acetic acid was used to adjust pH value of the solution to ~ 6.0 . Secondly, a three-electrode cell set up was used for electrochemical deposition, where ITO-coated glass plate, the platinum electrode and saturated calomel electrode (SCE) were taken as working electrode, counter electrode and reference electrode respectively. The distance between the anode and cathode was 2 cm and put the reference electrode close to the working electrode. Next, the electrochemical deposition was done under potentiostatic condition of stable DC voltage. The whole system was immersed in a water bath to keep the temperature of electrolyte constant. At the end of the growth duration, wash the ITO with deionized water to remove the presence of any ions. The as-deposited nanocrystals needed to be annealed at 400°C for 2 h in air atmosphere with the heating rate of 5°C min^{-1} .

2.3 Property characterization

X-ray diffraction (XRD) was carried out by using an X-ray diffractometer model D8 advance (Bruker) with $\text{Cu K}\alpha$ radiation ($\lambda = 0.154178 \text{ nm}$) at a scanning rate of 0.02°s^{-1} in the 2θ range from 5° to 70° . Field emission scanning electron microscopy (FESEM) experiments were performed on a Hitachi SU8010 electron microscope. The absorbance of prepared CuO film was measured by a UV–Vis spectrophotometer (UV-2550, Shimadzu, Japan).

Methyl blue (MB) is commonly adopted as a representative organic pollutant to evaluate the photocatalytic

performance of the samples. The dye solution was prepared by dissolving MB in de-ionized water with concentration of 12 mg L^{-1} . And the required amount of the photocatalyst ($1 \text{ cm} \times 1 \text{ cm}$) was added into it. Then the above suspension was exposed to light irradiation by a Xe lamp with the wavelength range from 200 nm to 800 nm. The solution with fixed amount was taken during the experiments every 30 min and was analyzed by a UV–Vis spectrophotometer (UV-2550, Shimadzu, Japan).

3 Results and discussion

3.1 Structural studies

XRD patterns of La-doped and undoped CuO films are shown in Fig. 1. XRD analysis reveals that CuO film and La-doped CuO film were comprised of monoclinic phase structure of CuO, namely, the planes (002), (111), (-202), (020), and (-113) at 2θ values of 35.49° , 38.91° , 49.10° , 53.60° and 61.77° , respectively, which all are in good agreement with JCPDS No.65-2309 (lattice constants

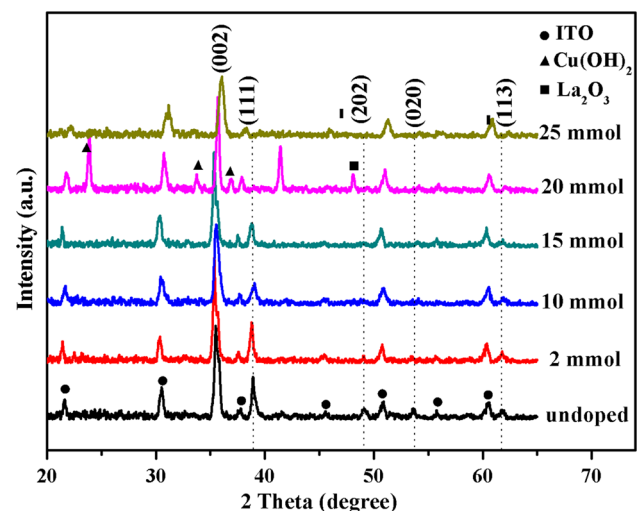


Fig. 1 XRD patterns of La-doped CuO nanosheets with different doping amount

$a = 4.662$, $b = 3.416$, $c = 5.118 \text{ \AA}$ and $\beta = 99.49$). When the doped amount of La^{3+} was less than 20 mmol, no diffraction peaks related to La_2O_3 and $\text{Cu}(\text{OH})_2$ were observed. It can be seen that the main diffraction peak (002) at 35.49° of CuO is shifted to lower angle with the increase of lanthanum doping and the La-doped CuO has a certain extent of peak broadening relative to the undoped, indicating lattice distortion in the CuO crystal structure. The phenomenon can be explained by the fact that the ionic radius of La^{3+} (1.08 \AA) [21] was larger than that of Cu^{2+} (0.73 \AA) [22]. When the doping amount exceeds 15 mmol, there are obvious impurity phase of La_2O_3 is observed in the XRD patterns and the major peak of CuO is shifted to higher angle, which demonstrates that excessive lanthanum tends to generate the oxides of La. The crystallite size of the samples are calculated using Scherrer's formula [23] and shown in Fig. 2.

$$D = \frac{k\lambda}{\beta \cos \theta} \tag{1}$$

where k is the shape factor (~ 0.89), λ is the wavelength of Cu $K\alpha$ radiation, θ is Bragg's angle of the peaks and β is the full width at half maximum (FWHM) of diffraction peak. The grain size increases dramatically at first from 16.83 to 26.60 nm. Then, when the amount of lanthanum doping is 10 mmol, the grain size is only 17.19 nm. The value can be got the highest with the doping amount of 15 mmol.

3.2 Morphological studies

The surface morphology and composition of the samples are determined by field emission scanning electron microscopy (FESEM) equipped with energy dispersive

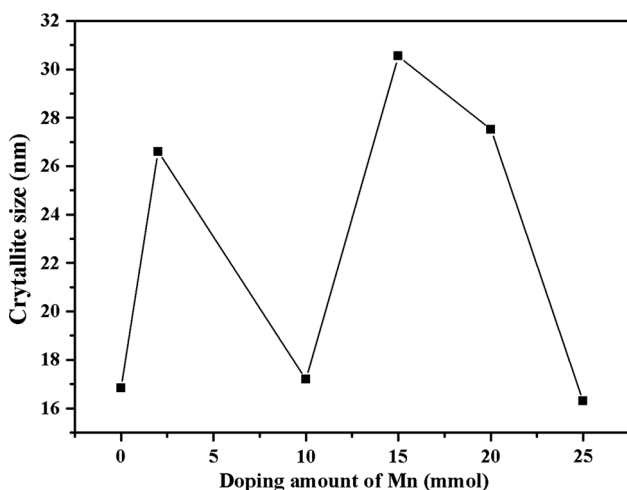


Fig. 2 Crystallite size of La-doped CuO along the major crystal face of (002)

spectroscopy (EDS) as shown in Fig. 3. In general, La^{3+} doping has much influence on the micromorphology of CuO. For pure CuO, irregular CuO nanoparticles aggregate to form petal-like structures with gaps. When the amount of lanthanum doping is 2 mmol, the size of CuO nanoparticles get moere uniform and the gaps decreased. With the La^{3+} increasing to 10 mmol, the connection between the particles is very compact and there is no any space on the surface of petals. When the doping amount is 15 mmol, petal-like structures disappear and forms cubic-like structures. Then, cubes gathers to produce flower-like structures. The detailed actual doping amount of La is given in Fig. 4. The EDS spectra of CuO presented in Fig. 4a shows the presence of Cu and O elements alone in the sample, from which we can see that atomic percent of O and Cu is 45.48–54.52 %, respectively. The actual mass percent of La can improve by doping more manganese element between the doping amount of 2–15 mmol. The ratio of metallic-ion/oxygen-ion is 1.20, 1.26, 1.38, 1.40, 14.8 and 1.30, respectively under the different doping amount, which demonstrates that there are much cation vacancies in crystal structure.

3.3 Optical studies

The photocatalytic activity of La-doped CuO nanostructures is examined through the photodegradation of MB in La-doped CuO aqueous suspensions under UV–Vis light irradiation. It can be seen from the Fig. 5 that La doping can greatly decrease absorption performance both in UV and the visible light region. The optical band gap energy (E_g) is calculated using the Eq. (2) [24]:

$$(\alpha h\nu)^{1/r} = B(h\nu - E_g) \tag{2}$$

where E_g is the band gap energy, B is a constant, ν is the frequency of the incident radiation, h is Planck's constant, α is the absorption coefficient, r is determined by the type of optical transition of a semiconductor. The band gap can be gotten by extrapolating the linear section of the plot of $(\alpha h\nu)^2$ versus $h\nu$ in the high absorption range and finding the intercept on the X-axis. The measured optical band gap E_g values are 1.25, 1.10, 1.30, 1.30, 1.15 and 1.10 eV, respectively with the increasing doping level. When the doping amount of La is only 2 mmol, slight red-shift behavior can be gotten in band gap comparing with the undoped sample because of the formation of impurity levels within the band gap of CuO due to La doping. Some defects brought from doping also can cause intragap defect states. However, with the continue increase of La doping, quantum confinement effect because of the decreased particle size can leads to the blue-shift band gap. When there are impurities such as La_2O_3 and $\text{Cu}(\text{OH})_2$ in samples, a slight shift of band gap to lower energies again.

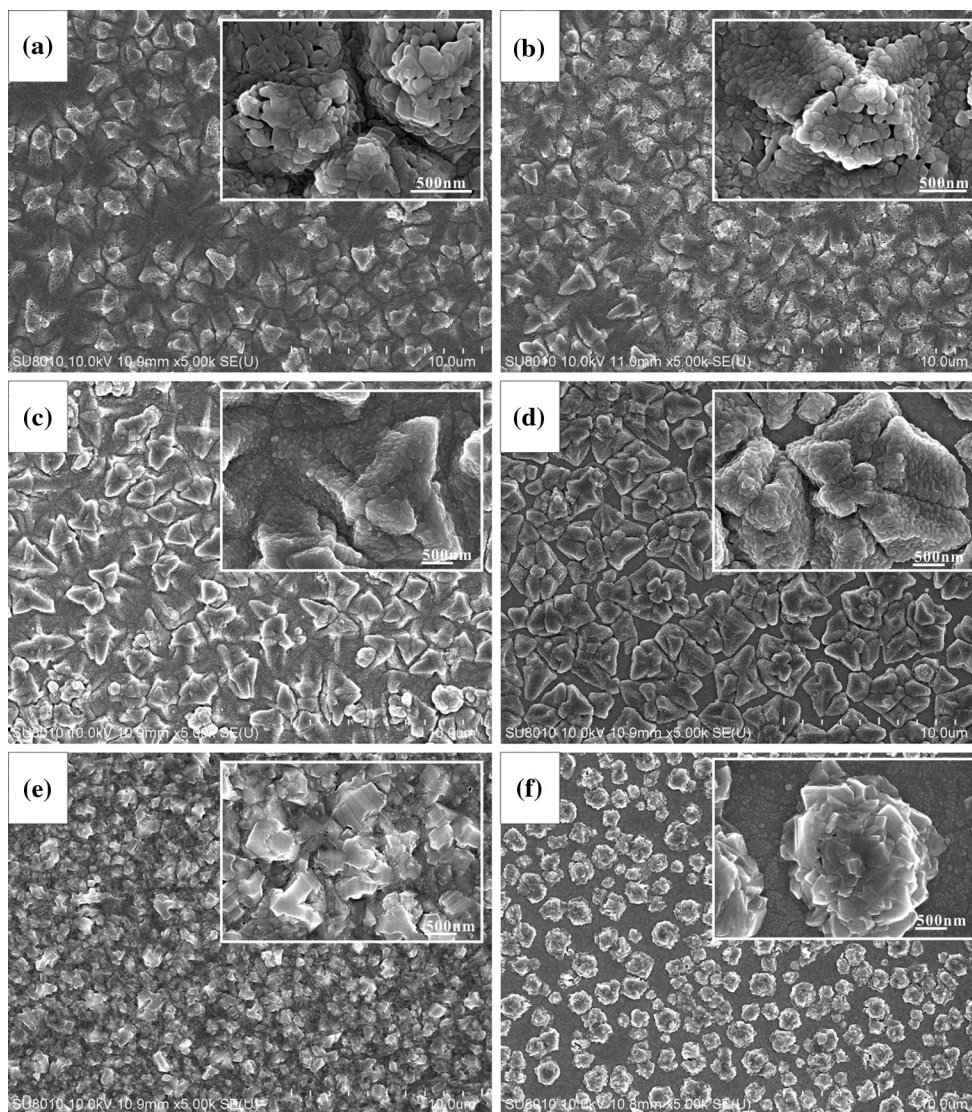


Fig. 3 FESEM images of undoped and La-doped CuO nanostructures **a** undoped, **b** 2 mmol, **c** 10 mmol, **d** 15 mmol, **e** 20 mmol, **f** 25 mmol

3.4 Photocatalytic studies

The photocatalytic activity of La-doped CuO nanostructures is examined through the photodegradation of MB in La-doped CuO aqueous suspensions under UV–Vis light irradiation. It can be seen from the Fig. 6 that La-doped CuO shows much higher photocatalytic activity than pure CuO nanosheets. The degradation of MB improves with the increase of dopant concentration. However, when La content is 5.78 wt%, the sample has the best photocatalytic performance whose photodegradation to MB can reach 90.9 %, which is 11.5 % higher than that in undoped CuO. Because lattice expansion would result in the increase of carrier mobility, which can effectively prevent the recombination of photogenerated electrons and holes. Ans a large

number of oxygen vacancies in the CuO crystal lattices and other lattice defects are prone to the oxidation center in photocatalytic reaction.

4 Conclusion

In summary, petal-like La-doped CuO nanostructures were successfully prepared by using electrodeposition method. XRD studies reveals La^{3+} is successfully doped into the CuO lattice. FESEM figures show that the doping amount has great influence on the morphology of samples. Comparing with the undoped samples, both red-shift and blue-shift behavior can be gotten in band gap which is between 1.10 and 1.30 eV. Synthesized La doped CuO demonstrate

Fig. 4 EDS results of undoped and La-doped CuO nanostructures **a** undoped, **b** 2 mmol, **c** 10 mmol, **d** 15 mmol, **e** 20 mmol, **f** 25 mmol

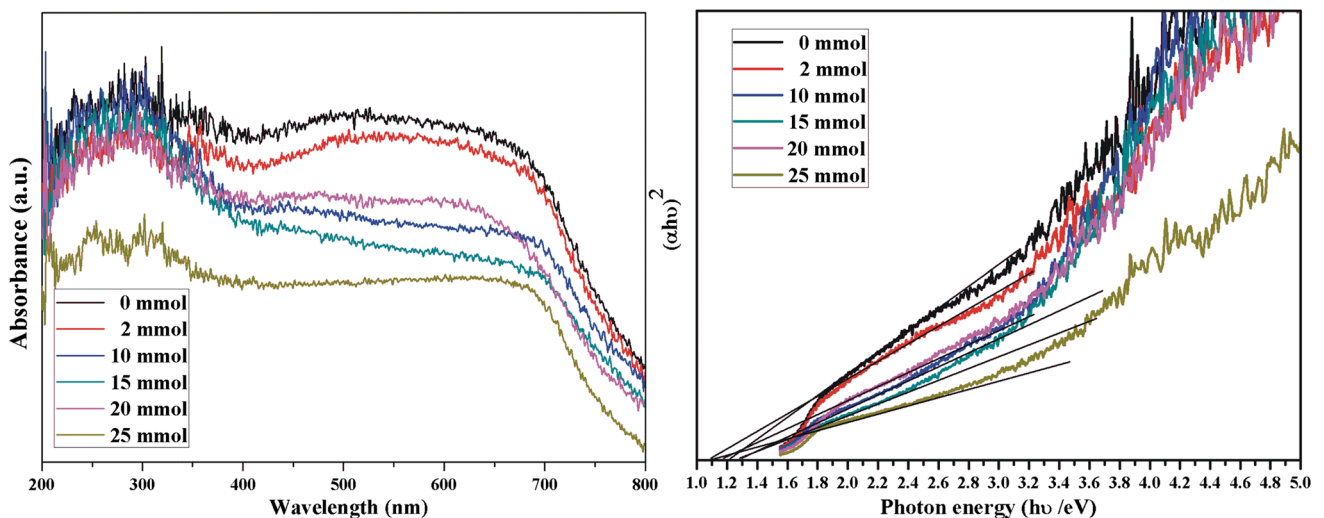
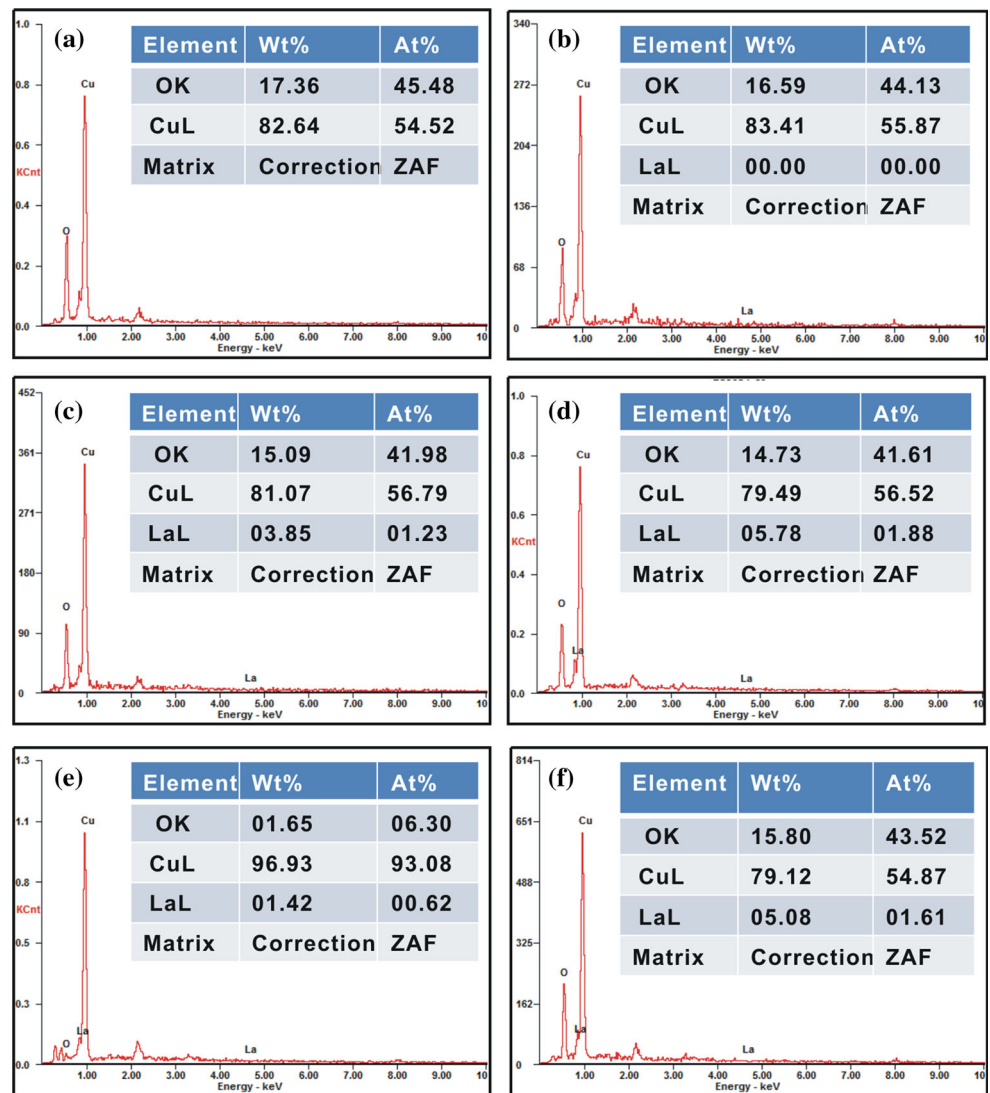


Fig. 5 UV–Vis absorption spectra (the left) and plot of $(\alpha hv)^2$ versus $h\nu$ (the right) of La-doped CuO with different doping amount

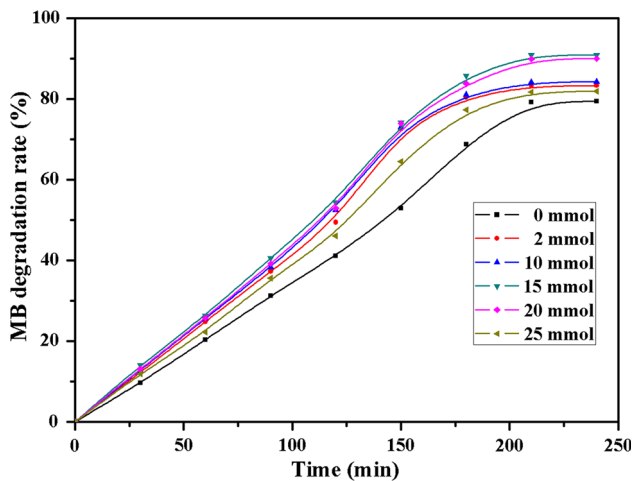


Fig. 6 MB degradation curves over undoped and La-doped CuO nanostructures

much enhancement in photocatalytic activity towards methylene blue, which demonstrate La-doped CuO films has excellent photocatalytic performance.

Acknowledgments This work is supported by Guangxi Experiment Centre of Science and Technology with open project: YXKT2014027. Another financial support is the Fundamental Research Funds for the Central Universities, China University of Geosciences (Wuhan, CUG120118). They are all gratefully appreciated.

References

- S. Anandan, S. Yang, Emergent methods to synthesize and characterize semiconductor CuO nanoparticles with various morphologies—an overview. *J. Exp. Nanosci.* **2**, 23–56 (2007)
- M.K. Song, S. Park, F.M. Alamgir, J. Cho, M. Liu, Nanostructured electrodes for lithium-ion and lithium-air batteries: the latest developments, challenges, and perspectives. *Mater. Sci. Eng. R Rep.* **72**, 203–252 (2011)
- C.H. Han, Z.Y. Li, J.Y. Shen, Photocatalytic degradation of dodecyl-benzenesulfonate over TiO₂-Cu₂O under visible irradiation. *J. Hazard. Mater.* **168**, 15–219 (2009)
- H. Ahmad, S.K. Kamarudin, L.J. Minggu, M. Kassim, Hydrogen from photo-catalytic water splitting process: a review. *Renew. Sustain. Energy Rev.* **43**, 599–610 (2015)
- S. Sonia, I.J. Annsi, P.S. Kumar, D. Mangalaraj, C. Viswanathan, N. Ponpandian, Hydrothermal synthesis of novel Zn doped CuO nanoflowers as an efficient photodegradation material for textile dyes. *Mater. Lett.* **144**, 127–130 (2015)
- A. Yildiz, Ş. Horzum, N. Serin, T. Serin, Hopping conduction in In-doped CuO thin films. *Appl. Surf. Sci.* **318**, 105–107 (2014)
- W.L. Gao, S.H. Yang, S.G. Yang, L.Y. Lv, Y.W. Du, Synthesis and magnetic properties of Mn doped CuO. *Phys. Lett. A* **375**, 180–182 (2010)
- P. Chand, A. Gaur, A. Kumar, U.K. Gaur, Structural and optical study of Li doped CuO thin films on Si (100) substrate deposited by pulsed laser deposition. *Appl. Surf. Sci.* **307**, 280–286 (2014)
- N.M. Basith, J.J. Vijaya, L.J. Kennedy, M. Bououdina, Structural, optical and room-temperature ferromagnetic properties of Fe-doped CuO nanostructures. *Physica E Low Dimens. Syst. Nanostruct.* **53**, 193–199 (2013)
- N.M. Basith, J.J. Vijaya, L.J. Kennedy, M. Bououdina, Structural, morphological, optical, and magnetic properties of Ni-doped CuO nanostructures prepared by a rapid microwave combustion method. *Mater. Sci. Semicond. Process.* **17**, 110–118 (2014)
- C. Mrabet, M.B. Amor, A. Boukhachem, M. Amlouk, T. Manoubi, Physical properties of La-doped NiO sprayed thin films for optoelectronic and sensor applications. *Ceram. Int.* (2016). doi:10.1016/j.ceramint.2015.12.144
- J. Liu, J. Jin, Z. Deng, S.-Z. Huang, Z.-Y. Hu, L. Wang et al., Tailoring CuO nanostructures for enhanced photocatalytic property. *J. Colloid Interface Sci.* **384**, 1–9 (2012)
- X.Y. Yu, R.X. Xu, C. Gao, T. Luo, Y. Jia, J.H. Liu et al., Novel 3D hierarchical cotton-candy-like CuO: surfactant-free solvothermal synthesis and application in As(III) removal. *ACS Appl Mater. Interfaces* **4**, 1954–1962 (2012)
- I. Ali, New generation adsorbents for water treatment. *Chem. Rev.* **112**, 5073–5091 (2012)
- X. Zhang, W. Shi, J. Zhu, D. Kharistal, W. Zhao, B. Lalia et al., High-power and high-energy-density flexible pseudocapacitor electrodes made from porous CuO nanobelts and single-walled carbon nanotubes. *ACS Nano* **5**, 2013–2019 (2011)
- Y.W. Zhu, T. Yu, F.C. Cheong, X.J. Xu, C.T. Lim, V.B.C. Tan et al., Large-scale synthesis and field emission properties of vertically oriented CuO nanowire films. *Nanotechnology* **16**, 88–92 (2005)
- C. Rossi, K. Zhang, D. Esteve, P. Alphonse, P. Tailhades, C. Vahlas, Nanoenergetic materials for MEMS: a review. *J. Microelectromech. Syst.* **16**, 919–931 (2007)
- S.B.B. Wang, C.H.H. Hsiao, S.J.J. Chang, K.T.T. Lam, K.H.H. Wen, S.C.C. Hung et al., A CuO nanowire infrared photodetector. *Sens. Actuators A Phys.* **171**, 207–211 (2011)
- L.P. Zhou, B.X. Wang, X.F. Peng, X.Z. Du, Y.P. Yang, On the specific heat capacity of CuO nanofluid. *Adv. Mech. Eng.* **2010**, 1–4 (2010)
- K.J. Choi, H.W. Jang, One-dimensional oxide nanostructures as gas-sensing materials: review and issues. *Sensors* **10**, 4083–4099 (2010)
- F.W. Wang, M. Xu, L. Wei, Y.J. Wei, Y.H. Hu, W.Y. Fang, C.G. Zhu, Fabrication of La-doped TiO₂ film electrode and investigation of its electrocatalytic activity for furfural reduction. *Electrochim. Acta* **153**, 170–174 (2015)
- Y.Q. Wang, T.T. Jiang, D.W. Meng, D.G. Wang, M.H. Yu, Synthesis and enhanced photocatalytic property of feather-like Cd-doped CuO nanostructures by hydrothermal method. *Appl. Surf. Sci.* **355**, 191–196 (2015)
- D. Sivalingam, J.B. Gopalakrishnan, J. Bosco, B. Rayappan, Structural, morphological, electrical and vapour sensing properties of Mn doped nanostructured ZnO thin films. *Sens. Actuators B Chem.* **166–167**, 624–631 (2012)
- J. Tauc, R. Grigorovici, A. Vancu, Optical Properties and electronic structure of amorphous germanium. *Phys. Status Solidi (b)* **15**, 627–637 (1966)